Available online at www.sciencedirect.com

ScienceDirect

Procedia Structural Integrity 64 (2024) 409–417

Structural Integrity Procedia

www.elsevier.com/locate/procedia

SMAR 2024 – 7th International Conference on Smart Monitoring, Assessment and Rehabilitation of Civil Structures

Mixed-Mode Cohesive Failure of CFRP to Steel and Fe-SMA to Steel Bonded Joints

Niels Pichler[a,b]*, Lingzhen Li[a,b,d], Wandong Wang[c], Masoud Motavalli[a]

[a]*Empa, Swiss Federal Laboratories for Materials Science and Technology, 8600 Dübendorf,Switzerland*
[b]*Institute of Structural Engineering, Department of Civil, Environmental and Geomatic Engineering,ETH Zürich, 8093, Zürich, Switzerland*
[c]*School of Aeronautics, Northwestern Polytechnical University; P.R. China*
[d]*The Hong Kong Polytechnic University, Hong Kong, China*

Abstract

The integrity of carbon fibre reinforced polymers (CFRP)-to-steel and iron-based shape memory alloys (Fe-SMA)-to-steel adhesively bonded structural strengthening patch must be maintained to ensure a durable application. The influence of the adhesive thickness and adherend material behavior on the joint fracture has been well documented. The influence of mode-mixity has yet to be investigated and is studied experimentally and analytically in this study. In engineering applications, bonded strengthening patch, located in the shear span, may be subject to mixed-mode loading. Lap-shear tests involving mixed-mode fracture of bonded CFRP and Fe-SMA were conducted. The mode-mixity was introduced via an eccentricity between the loading axis and the adhesive plane. Furthermore, a novel theoretical model has been developed considering (i) adherend material behavior and (ii) mode-mixity. Experiments show that loading eccentricity decreases the joint capacity, up to 70% for CFRP and 32% for Fe-SMA. The theoretical analysis shows this difference is caused by the Fe-SMA material nonlinearity. The local mixity contains more Mode II in the Fe-SMA case than the CFRP case. Fe-SMA yielding mitigates the development of opening forces at the crack tip. These findings hold significant meaning relative to the structural resilience and robustness of joints. A strengthening solution employing Fe-SMA can benefit from material ductility to hinder the influence of loading eccentricity or misalignment of structural surfaces after damage.

Keywords: Iron-based shape memory alloy; Bonded joint; Mixed-mode failure; Modelling

* Corresponding author.
E-mail address: niels.pichler@empa.ch

10.1016/j.prostr.2024.09.277

1. Introduction

Iron-based shape memory alloy (Fe-SMA) exhibits significant potential as a retrofit, strengthening, and repair solution for maintaining existing structures. Adhesively bonding self-prestressing Fe-SMA strips to a damaged member can substantially increase its fatigue life (Li et al., 2023c; Wang et al., 2023, 2021). Moreover, adhesive bonding provides a straightforward method to seamlessly transfer prestress from the Fe-SMA to the damaged member without introducing additional stress concentrations. However, its application requires a thorough understanding of its major failure mode, i.e., debonding. Pure Mode II fracture of Fe-SMA bonded joints has been extensively studied both experimentally (Li et al., 2023d; Wang et al., 2021) and theoretically (Li et al., 2023b). These works demonstrated that the nonlinear stress-strain relationship of Fe-SMA significantly influences bond behavior, such as joint bond strength, especially with tough adhesives. Investigations into pure Mode I fracture have also been conducted, revealing a similar effect (Pichler et al., 2024).

To date, mixed-mode failure has not been thoroughly investigated, despite representing the majority of loading cases in practical applications. Given the understanding of pure mode (I and II) failure cases, exploring mixed-mode failures becomes pertinent. The lack of understanding of mixed mode failure of adhesively bonded Fe-SMA joints poses potential risks in terms of ensuring structural integrity. However, the nonlinear material behavior of Fe-SMA poses challenges; preliminary numerical investigations suggest that the commonly used mixed-mode bending test (D30 Committee, 2019.) is impractical, leading to large displacements and primarily Mode I dominated fracture. A recent study on mixed-mode bond behavior of CFRP-to-steel joints proposes an alternative test by adapting the double lap-shear test (Zhao et al., 2023). This study demonstrated that the impact of mode-mixity on bond strength is significant even for small peel angles, emphasizing the importance of studying it. However, proper quantification of the Mode I contribution is lacking, and the commonly defined mode-mixity cannot be obtained. In the present work, experiments loading Fe-SMA to steel and CFRP to Steel joints are tested under mixed-mode by modifiying the commonly used single lap-shear test (Doroudi et al., 2020; Fernando et al., 2014). To further the understanding of the failure phenomena and the implication of Fe-SMA material behavior, an analytical model is derived and used to quantify the mode-mixity at failure initiation.

2. Material and method

The mode mixity is introduced via an offset between the loading axis and the sample. For each material type (Fe-SMA and CFRP), two samples were tested per offset and four offsets (0mm, 8mm, 12mm, 20mm) were tested.

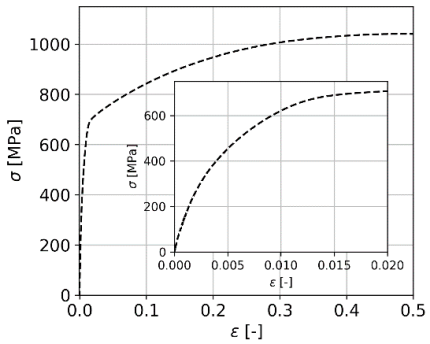

Figure 1:Fe-SMA stress-strain behavior

2.1. Material properties

The Fe-SMA strips, provided by re-fer AG, were nominally 1.5mm thick, 50mm wide, and 600mm long. Before delivery, these strips underwent a prestrain of 2% at the manufacturing facility and machined to meet specific

dimensions. The mechanical characteristics of the Fe-SMA were assessed following the methodology in (Mohri et al., 2022). The resulting stress-strain relationship is illustrated in Figure 1.

For the CFRP strip, supplied by S&P Clever Reinforcement Company AG (S&P 150/2000), rolls with a thickness of 1.4mm and a width of 50mm were provided and subsequently cut to the required length. SikaPower 1277 adhesive was employed in the bonding process, a material previously utilized in Mode I and Mode II fracture tests of Fe-SMA bonded joints (Li et al., 2023d; Pichler et al., 2024). This adhesive exhibits nonlinear characteristics with ductile behavior and an initial Young's modulus of E = 1,952 MPa (Li et al., 2023d). A summary of all material properties is presented in Table 1.

Table 1: Material properties and dimension

Material	E modulus [MPa]	Thickness [mm]	Width [mm]
Fe-SMA	150'810	1.5	50
S&P 150/2000 CFRP	155'000	1.4	50

2.2. Sample preparation

The bonding surfaces of the support plates and Fe-SMA strips underwent a cleaning process with acetone-soaked cotton wipes until no traces of grease or oxides could be observed. Subsequently, the bonding surfaces were grit-blasted and cleaned once again with acetone. The preparation of the CFRP strips involved a simpler cleaning process using acetone wipes only.

To make a precrack, a Teflon strip was wrapped around the adherend (Fe-SMA and CFRP) 200mm away from the strip's end, as illustrated in Figure 2. Subsequently, adhesive was applied to the adherend and the bonding surface of the support plates. A 0.5mm spacer wrapped in Teflon tape was used to control the thickness, and weights were placed on the strip to remove excess adhesive and achieve a minimal adhesive thickness of 0.5mm. After 24 hours, the weights were removed, and the samples were cured in a controlled environment room (temperature T = 20°C, relative humidity RH = 50%) for a minimum of two weeks.

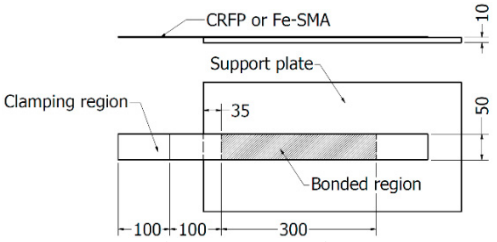

Figure 2: Test sample

To prevent direct contact between the CFRP and the clamp initiating damage potentially leading to delaminaiton, loading tabs made of aluminum were bonded to the clamping region of the CFRP samples using 3M Scotch-Weld EC-9323 adhesive. The spacers and Teflon precrack strip were then removed, and the sample was prepared for digital image correlation (DIC). White paint was applied in two passes, and after drying, a black speckled pattern was applied using a stamp with a 0.013" dot size.

2.3. Test setup

Figure 3a) shows of the experimental setup utilized. The sample, along with its clamping setup, is positioned on spacer plates highlighted in the figure. These spacer plates come in thicknesses of 8 mm, 12 mm, and 20 mm. To adjust the setup, spacers can be removed, allowing the base plate to descend and introducing an offset equivalent to the removed spacer's thickness (0 mm, 8 mm, 12 mm, 20 mm) between the hydraulic jack and the sample. Spacers are also placed under the clamp to ensure a horizontal loading axis. For clamping, the loading end of the sample is deformed to reach the clamp introducing the initial opening. The load is applied using the hydraulic jack in a

displacement-controlled manner. The loading rates are set at 0.02 mm/s for Fe-SMA samples and 0.003 mm/s for CFRP samples to maintain consistency with prior research (Li et al., 2023b).

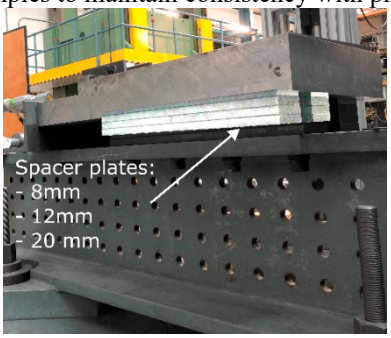

(a)

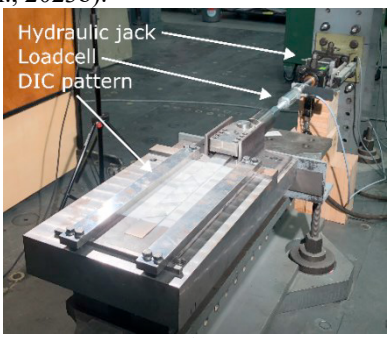

(b)

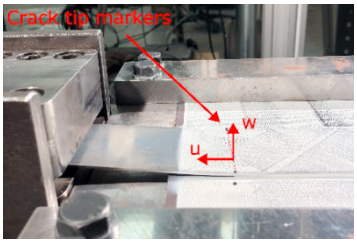

(c)

Figure 3: a) Spacer plates underneath the test setup; b) Loading setup and DIC pattern; c) Crack tip markers and measured variables.

Figure 3b) illustrates the measurement system employed in the tests. Force measurement is conducted using a 150 kN load cell. Two DIC cameras are strategically positioned to capture the entire bonded strip along with its surroundings. The complete displacement field is measured throughout the test.

To gauge crack tip displacements, additional markers are applied to the sample, as shown in Figure 3c). The relative out-of-plane crack opening, w, and displacement in the loading direction, u, are extracted at two Gauss points along the line connecting both markers, as detailed in (Li et al., 2023d), before averaging. The displacement in the loading direction is corrected to account for geometric effects introduced by the offset, providing a measurement of the crack slip at the crack tip.

The Fe-SMA was not activated in this study in order to limit the number of influencing parameters. A recent investigation on the influence of activation on the pure Mode II joint behavior showed a limited influence (Li et al., 2023). The investigation on mixed-mode CFRP bonded joints (Zhao et al., 2023) found that mixed-mode debonding behavior certainly reduces the bond capacity. Such a behavior is expected to occur in Fe-SMA bonded joints. Therefore, the current study focuses on the effect of mixed-mode, while leaving the influence of activation for further investigations.

3. Analytical model

3.1. Nonlinear Timoshenko beams

To model the experiment, both the unbonded and bonded region are considered as depicted in Figure 4a). In the bonded region, the force and moment equilibrium equations are given by (Gao and Su, 2015):

$$-P - N\frac{dw}{dx} + \frac{dM}{dx} - \tau\frac{h}{2} = 0 \quad (1)$$

$$q + \frac{dP}{dx} = 0 \quad (2)$$

$$\frac{dN}{dx} - \tau = 0 \quad (3)$$

where P is the transverse force, N is the longitudinal force, and M is the bending moment acting on the infinitesimal beam element of height h, represented in Figure 4b). The distributed transverse loading is denoted σ and the distributed shear loading is denoted τ.

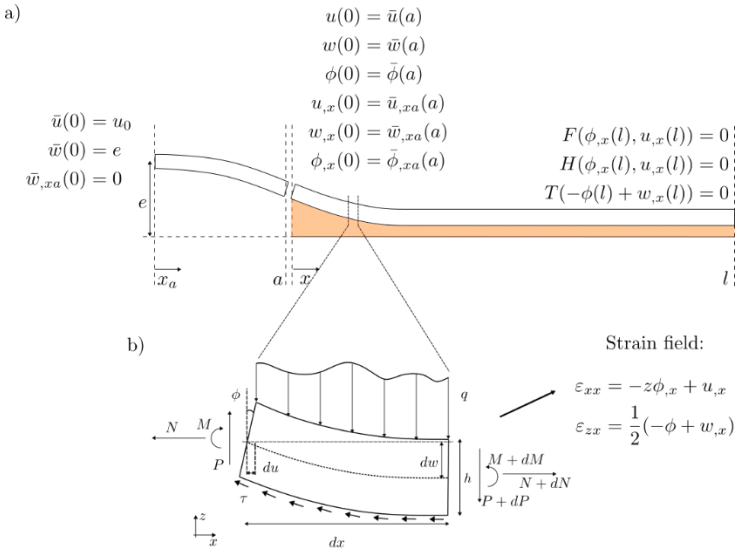

Figure 4: a) Schematic of the model, boundary and continuity conditions; b) Loaded infinitesimal beam segment.

Assuming a generic stress-strain relationship $\sigma_{xx} = S_1(\varepsilon_{xx})$ and $\sigma_{zx} = S_2(\varepsilon_{zx})$ the following beam constitutive behavior relating internal load and displacement can be obtained through integration of the stress fields over the beam height.

$$M = \int_{-\frac{h}{2}}^{\frac{h}{2}} -z\sigma_{xx}dA = \int_{-\frac{h}{2}}^{\frac{h}{2}} -zS_1\left(-z\phi_{,x} + u_{,x}\right)dA = F\left(\phi_{,x}, u_{,x}\right) \quad (4)$$

$$P = \int_{-h/2}^{h/2} -\sigma_{zx}dA = \int_{-h/2}^{h/2} -zS_2\left(0.5\left(-\phi + w_{,x}\right)\right)dA = T(-\phi + w_{,x}) \quad (5)$$

$$N = \int_{-h/2}^{h/2} -\sigma_{xx}dA = \int_{-h/2}^{h/2} -zS_1(-z\phi_{,x} + u_{,x})dA = H(\phi_{,x}, u_{,x}) \quad (6)$$

Therefore, the equilibrium equations (1)(2)(3) are given by:

$$\frac{\partial F}{\partial \phi_{,x}}\phi_{,xx} + \frac{\partial F}{\partial u_{,x}}u_{,xx} - Hw_{,x} - T - \tau\frac{h}{2} = 0 \quad (7)$$

$$\frac{dT}{d\alpha}\left(-\phi_{,x} + w_{,xx}\right) + q = 0 \quad (8)$$

$$\frac{\partial H}{\partial \phi_{,x}}\phi_{,xx} + \frac{\partial H}{\partial u_{,x}}u_{,xx} - \tau = 0 \quad (9)$$

The functions F and H are assessed across a grid of $\phi_{,x}, u_{,x}$, and T over a range of $\alpha = 0.5\left(-\phi + w_{,x}\right)$, employing trapezoidal integration of the corresponding stress profiles. Bivariate splines are used to interpolate the assessed values of F and H, while a cubic spline is employed for T.

3.2. Boundary conditions

In order to use the differential equation system, the loading and boundary conditions need to be defined. Therefore, the adhesive layer is modelled with a simple Cohesive Zone Model (CZM) that interpolates between well-established pure mode behaviors. The behavior in pure Mode I is described by $\tau_I(\delta_1)$, where δ_1 denotes the crack tip opening, and in pure Mode II by $\tau_{II}(\delta_2)$, where δ_2 represents the crack tip slip. The magnitude of mixed-mode displacement is calculated as $\delta_m = \sqrt{\delta_1 + \delta_2}$, and the mixed-mode angle is defined as $\theta = \text{atan}\left(\frac{2\delta_2}{\delta_1 + |\delta_1|}\right)$. The magnitude of mixed-mode stress, denoted by σ is determined through interpolation in radial coordinates using:

$$\sigma = \tau_I(\delta_m) + \left(\tau_{II}(\delta_m) - \tau_I(\delta_m)\right)\left(\frac{2|\theta|}{\pi}\right)^n \quad (10)$$

Figure 5: Pure Mode cohesive behaviors

A trapezoidal bond-slip behavior measured in pure Mode II, as documented in (Li et al., 2023d), and employing a trapezoidal shape with a tail for the traction-separation behaviour shown in Figure 5 are used. While other CZMs exist (Dimitri et al., 2015; Goutianos, 2017; Van Den Bosch et al., 2006), the proposed approach has the appeal of simplicity and accounts for different shapes in Mode I and Mode II.
The offset and imposed displacements are imposed as boundary conditions along with the appropriate continuity and load conditions displayed in Figure 4. Finally, a numerical solver solves the differential equation system.

4. Results and discussion

4.1. Load-displacement curves

For a solution to the equations with a specific imposed displacement $\bar{u}(0) = u_0$, as depicted in Figure 4, the normal reaction load N can be expressed as $N = H(\phi_{,x}(0), u_{,x}(0))$. The crack tip opening is denoted by $w(0)$, and the slip of the upper side of the beam at the crack tip is given by $u_{top} = u(0) - \phi(0)\frac{h}{2}$. By computing multiple solutions for an increasing series of applied displacement $\bar{u}(0) = u_0$, it is feasible to predict the load-displacement curves. The comparison between the experimental load-displacement curves and the model's predictions is presented in Figure 6.

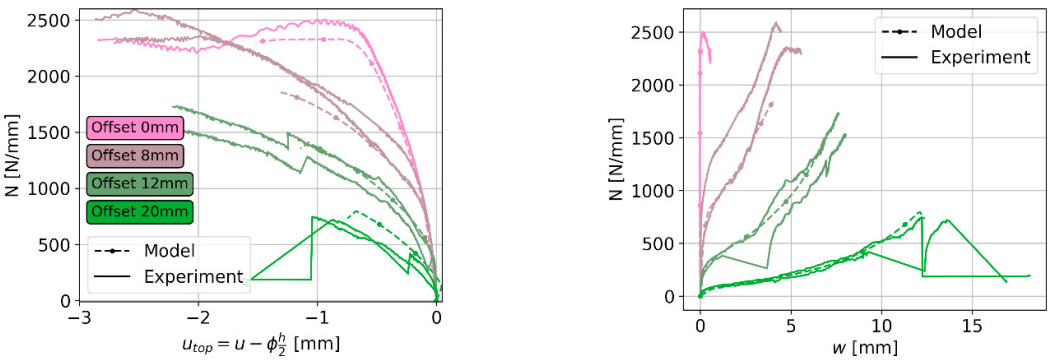

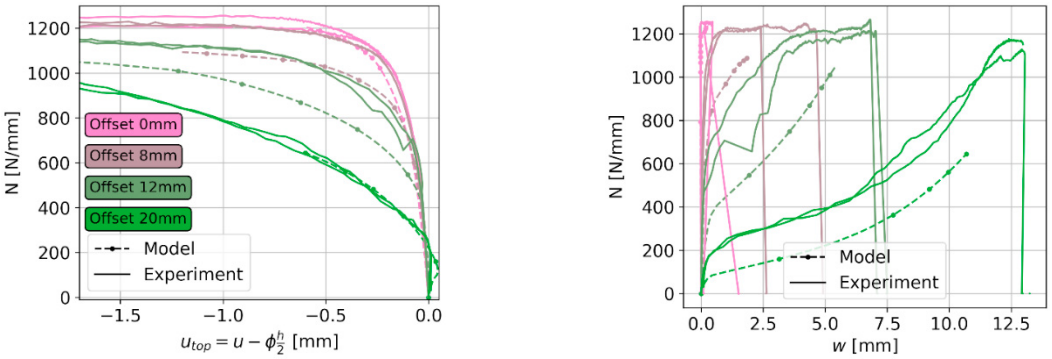

c) d)

Figure 6: Load displacement curves, experiment and modelling; a) slip at the crack tip, CFRP; b) opening at the crack tip, CFRP; c) slip at the crack tip, Fe-SMA; d) opening at the crack tip, Fe-SMA

The model captures the underlying physical trends observed in the experiments. While not entirely precise, it effectively predicts the influence of the offset on the load-displacement curves for both material types. As the offset increases, there is a noticeable drop in load, accompanied by an increase in the opening of the crack tip. This drop in load is particularly pronounced with the CFRP material.

To enhance the accuracy of the model predictions, adjustments could be made to the CZM formulation to better represent the physical mixed-mode failure of the adhesive layer. However, such refinements are beyond the scope of the present work. The current model serves to provide a qualitative description, offering insights into the effect of mode mixity on the failure process of bonded strengthening patches

4.2. Mode Partitioning

With the 20 mm offset, the CFRP joint reached a maximum load only 30% of its pure Mode II bond capacity, while the Fe-SMA is still reaching 68% of its pure Mode II bond capacity.

The difference in local mode-mixity should be considered. By computing the work of the crack tip forces in the opening and transverse direction, the Mode I and Mode II contributions can be readily obtained. Equations (11) and (12) are applied to modeling results spanning the whole initiation process. Finally, the mode mixity is commonly defined as $\psi = \frac{G_{II}}{G_I + G_{II}}$, where:

$$G_I = \int_{\delta_1(u_0=0)}^{\delta_1(u_0=u_{init})} q d\delta_1 \quad (11)$$

$$G_{II} = \int_{\delta_2(u_0=0)}^{\delta_2(u_0=u_{init})} \tau d\delta_2 \quad (12)$$

Figure 7 shows in black the path taken by the crack tip in the δ_1-δ_2-σ space for the 8 mm offset case, using the average CZM parameters obtained for each adherend type. The contribution of each mode is shown in the δ_1-σ and δ_2-σ planes, highlighting the difference in mixity between the two cases.

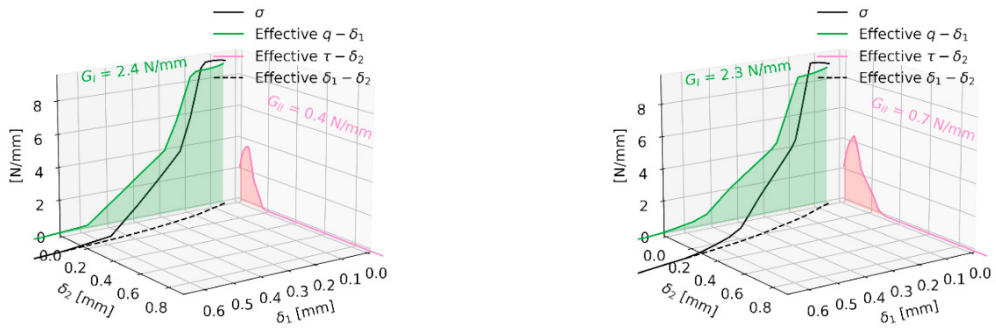

(a) (b)

Figure 7: Fracture energy decomposition. a) CFRP; b) Fe-SMA

Table 2 shows the average local mixity for each experiment type. From this table, it is clear that the sharper drop in mixity for the CFRP samples is the reason for the decreased load. The adhesive, sample geometry, Young's modulus, offsets being the same for the two material tested, it is concluded that the nonlinearity of the Fe-SMA is the cause for the reduced sensitivity to offset.

Table 2: Mode mixity at the crack tip

Offset	20 mm	12 mm	8 mm	0 mm
Fe-SMA	0.036	0.075	0.225	1
S&P 150/2000 CFRP	0.015	0.050	0.140	1

5. Conclusion

In this study, the mixed-mode fracture of CFRP-to-steel and Fe-SMA-to-steel is investigated experimentally and theoretically. The following conclusions can be drawn:

- The lap-shear test setup is adapted to produce mixed-mode loading of the bonded joint by adjusting the loading eccentricity. Two series of experiments are carried out testing two types of adherends. Experimental results show a significant reduction in the bond capacity with increasing loading eccentricity.
- A new theoretical framework is proposed to consider the adherend material behavior and its interaction with the adhesive layer. It yields a new analytical model to consider mixed-mode loading in lap-shear tests. Using a reasonable estimate for the mixed-mode cohesive behavior of the adhesive, the model shows good agreement with experimental observations.
- Investigation supported by the calibrated proposed model reveals that the mode mixity at the crack tip is dependent on the adherend material property. The nonlinear behavior of the Fe-SMA hinders the impact of loading eccentricity on the decrease of mixity.

Acknowledgements

The authors would like to acknowledge the financial support of the Swiss National Foundation, SNSF (Grant No. 200021_192238), and re-fer AG for providing the material used for this work.

References

D30 Committee, n.d. Test Method for Mixed Mode I-Mode II Interlaminar Fracture Toughness of Unidirectional Fiber Reinforced Polymer Matrix Composites. ASTM International. https://doi.org/10.1520/D6671_D6671M-19

Dimitri, R., Trullo, M., De Lorenzis, L., Zavarise, G., 2015. Coupled cohesive zone models for mixed-mode fracture: A comparative study. Engineering Fracture Mechanics 148, 145–179. https://doi.org/10.1016/j.engfracmech.2015.09.029

Doroudi, Y., Fernando, D., Zhou, H., Nguyen, V.T., Ghafoori, E., 2020. Fatigue behavior of FRP-to-steel bonded interface: An experimental study with a damage plasticity model. International Journal of Fatigue 139, 105785. https://doi.org/10.1016/j.ijfatigue.2020.105785

Fernando, D., Yu, T., Teng, J.G., 2014. Behavior of CFRP Laminates Bonded to a Steel Substrate Using a Ductile Adhesive. J. Compos. Constr. 18, 04013040. https://doi.org/10.1061/(ASCE)CC.1943-5614.0000439

Gao, X.-L., Su, Y.-Y., 2015. An analytical study on peeling of an adhesively bonded joint based on a viscoelastic Bernoulli–Euler beam model. Acta Mech 226, 3059–3067. https://doi.org/10.1007/s00707-015-1357-8

Goutianos, S., 2017. Derivation of Path Independent Coupled Mix Mode Cohesive Laws from Fracture Resistance Curves. Appl Compos Mater 24, 983–997. https://doi.org/10.1007/s10443-016-9568-2

Li, L., Chatzi, E., Czaderski, C., Ghafoori, E., 2023a. Influence of activation temperature and prestress on behavior of Fe-SMA bonded joints. Construction and Building Materials 409, 134070. https://doi.org/10.1016/j.conbuildmat.2023.134070

Li, L., Chatzi, E., Ghafoori, E., 2023b. Debonding model for nonlinear Fe-SMA strips bonded with nonlinear adhesives. Engineering Fracture Mechanics 282, 109201. https://doi.org/10.1016/j.engfracmech.2023.109201

Li, L., Wang, S., Chen, T., Chatzi, E., Heydarinouri, H., Ghafoori, E., 2023c. Fatigue strengthening of cracked steel plates with bonded Fe-SMA strips. ce papers 6, 380–384. https://doi.org/10.1002/cepa.2559

Li, L., Wang, W., Chatzi, E., Ghafoori, E., 2023d. Experimental investigation on debonding behavior of Fe-SMA-to-steel joints. Construction and Building Materials 364, 129857. https://doi.org/10.1016/j.conbuildmat.2022.129857

Mohri, M., Ferretto, I., Leinenbach, C., Kim, D., Lignos, D.G., Ghafoori, E., 2022. Effect of thermomechanical treatment and microstructure on pseudo-elastic behavior of Fe–Mn–Si–Cr–Ni-(V, C) shape memory alloy. Materials Science and Engineering: A 855, 143917. https://doi.org/10.1016/j.msea.2022.143917

Pichler, N., Wang, W., Motavalli, M., Taras, A., Ghafoori, E., 2024. Mode I fracture analysis of Fe-SMA bonded double cantilever beam considering nonlinear behavior of the adherends. Engineering Fracture Mechanics 295, 109789. https://doi.org/10.1016/j.engfracmech.2023.109789

Van Den Bosch, M.J., Schreurs, P.J.G., Geers, M.G.D., 2006. An improved description of the exponential Xu and Needleman cohesive zone law for mixed-mode decohesion. Engineering Fracture Mechanics 73, 1220–1234. https://doi.org/10.1016/j.engfracmech.2005.12.006

Wang, S., Li, L., Su, Q., Jiang, X., Ghafoori, E., 2023. Strengthening of steel beams with adhesively bonded memory-steel strips. Thin-Walled Structures 189, 110901. https://doi.org/10.1016/j.tws.2023.110901

Wang, W., Li, L., Hosseini, A., Ghafoori, E., 2021. Novel fatigue strengthening solution for metallic structures using adhesively bonded Fe-SMA strips: A proof of concept study. International Journal of Fatigue 148, 106237. https://doi.org/10.1016/j.ijfatigue.2021.106237

Zhao, J., Fang, J., Yang, Y., Zhang, S., Biscaia, H., 2023. Experimental study on mixed mode-I & II bond behavior of CFRP-to-steel joints with a ductile adhesive. Thin-Walled Structures 184, 110532. https://doi.org/10.1016/j.tws.2023.110532